NANO · MICRO small
www.small-journal.com

Black Phosphorus Nanosheets Passivation Using a Tripeptide

Huaying Wang, Kuan Hu, Zhe Li, Chan Wang, Min Yu, Zigang Li, and Zhou Li**

In the past several years, 2D black phosphorus (BP) has captured the research community's interest because of its unique electronic, photonic, and mechanical properties. However, the intrinsic instability of BP limits its preservation and practical application. Despite kinds of BP passivation strategies being well-documented, the use of metal ligand coordination or polymer modification may have potential long-term detrimental effects on human bodies. Here, a tailored tripeptide Fmoc-Lys-Lys-Phe (Fmoc-KKF) is synthesized for surface modification of BP nanosheets. Compared with bare BP with rapid degradation, the BP@FKK complex exhibits excellent stability, thereby significantly increasing the life span. Significantly, the BP@FKK shows favorable cell compatibility and enhanced cellular uptake compared to the bare BP.

The 2D material black phosphorus (BP), with a p-type direct bandgap (≈0.3–2.0 eV), has received great attention because of its unique electronic and optical properties,[1] which has many promising applications in electrochemical energy storage[2] and optoelectronic devices.[1c,e,3] Recent studies have reported that few-layer BP sheets or a single-layer phosphorene could be exfoliated from bulk BP materials because of their strong in-plane bonds and the weak van der Waals interlayer interaction.[4] With the advent of the ultra-small size BP, the applicable research field of this multifunctional material has been gradually widened. Very recently, BP has generated new opportunities for drug delivery, bioimaging, and further therapeutics due to its persistence of fluorescent intensity, low cytotoxicity, and high biocompatibility.[5] Compared with other 2D materials such as graphene and MoS_2, BP has much greater specific surface area due to its puckered lattice configuration, which can improve its drug loading ability.[5b,6] In addition, there is promising potential for nanoscale BP to be applied to photothermal therapy (PTT), because both BP nanoparticles and BP quantum dots (QDs) show broad absorptions across the entire visible light region.[5b,d,e][7]

In spite of these excellent properties, a tremendous challenge limiting the application of BP is its easy oxygenation.[8] The weak stability of BP under ambient conditions resulting in its rapid degradation both in vitro and in vivo, as a result, the potential electrochemical and biomedical applications of BP are further hindered. Thus, preventing the reaction between BP and oxygen in ambient environment is vital to maintain the stability, but implementing this in practical applications remains a great challenge. Many strategies such as capping layer protection,[8d,9] metal-ion modification,[6,10] covalent aryl diazonium functionalization,[11] and ligand surface coordination[12] have been suggested to improve the stability of BP.[9b,10–12] However, all these modification reagents are not bio-original, which may possess degradation problems in vivo or potential long-term detrimental effect on human bodies.[6] In this regard, a bio-original, and bioresorbable reagent, which can be selectively bound to BP, is urgently needed. Oligopeptides, due to their abundant sequences and possible secondary structures, as well as their inherent low-toxic nature, are most promising candidates to improve the stability of BP.

As known, BP has a puckered honey comb structure. Every phosphorus atom in each layer of BP has three single electrons and one lone pair electrons.[13] These single electrons are covalently bonded to the other three adjacent phosphorus atoms. The exposed lone pair electrons can irreversibly react with oxygen to form oxidized phosphorus species.[8c,d] In this study, we designed a tripeptide Fmoc-KKF (hereinafter FKK, unless otherwise stated) for modification of BP nanosheets. Herein, these lone pair electrons were occupied by peptides, FKK, to prevent the reaction between phosphorus and oxygen ultimately retarding degradation of BP.[11,12] According to the

H. Y. Wang, Dr. K. Hu, Z. Li, C. Wang, Dr. M. Yu, Prof. Z. Li
CAS Center for Excellence in Nanoscience
Beijing Key Laboratory of Micro-nano Energy and Sensor
Beijing Institute of Nanoenergy and Nanosystems
Chinese Academy of Sciences
Beijing 100083, China
E-mail: zli@binn.cas.cn
Dr. K. Hu, Z. Li, Prof. Z. Li
School of Nanoscience and Technology
University of Chinese Academy of Sciences
Beijing 100049, China
Dr. K. Hu, Z. Li, Prof. Z. Li
Center on Nanoenergy Research
School of Physical Science and Technology
Guangxi University
Nanning 530004, China
Prof. Z. G. Li
State Key Laboratory of Chemical Oncogenomics
School of Chemical Biology and Biotechnology
Shenzhen Graduate School
Peking University
Shenzhen 518055, China
E-mail: lizg@pkusz.edu.cn
The ORCID identification number(s) for the author(s) of this article can be found under https://doi.org/10.1002/smll.201801701.

DOI: 10.1002/smll.201801701

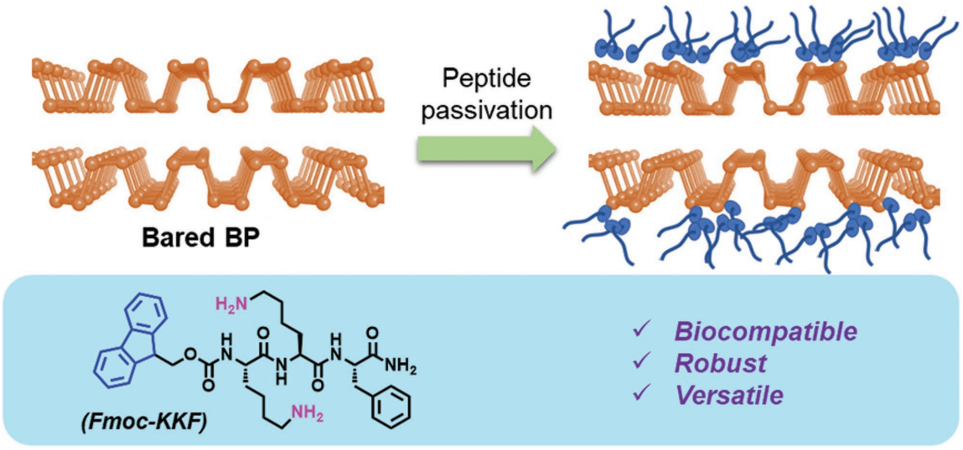

Scheme 1. Schematic illustration for structures of BP and FKK. The merits of the peptide passivation of BP were shown.

structure of BP and FKK (showed in **Scheme 1**), we assume that FKK interacts with BP via the π–p interaction of the benzene rings of Phe and Fmoc in FKK and lone pair electrons of BP or through the electrostatic interaction between NH_2- of Lys in FKK and lone pair electrons of BP. Morphology and spectrum characterizations were performed to detect the modification effect.

The BP nanosheets were produced by a liquid phase exfoliation method from bulk BP as reported previously.[4b,14] The tripeptides FKK were purchased commercially. The BP nanosheets dispersion in N-methyl-2-pyrrolidone (NMP) was mixed with FKK at room temperature for 4 h to generate the BP@FKK nanosheets. The excess free FKK in the original BP@FKK nanosheets mixture was removed by centrifugation. In order to find the appropriate modification effect, different mixing ratio of BP and FKK had been tested. Spectrum characterizations of BP nanosheets were analyzed to verify the modification of FKK on the surface of BP, and to examine the physicochemical properties of BP after FKK modification (**Figure 1**). The Raman scattering spectrum of bare BP, $BP@FKK_{(10)}$ (mass ratio, 1:10), and $BP@FKK_{(100)}$ (mass ratio, 1:100) nanosheets is displayed in Figure 1A. The three typical BP Raman peaks were at 360.9, 438.4, and 466.5 cm^{-1} corresponding to the A^1_g, B_{2g}, and A^2_g vibrational modes of P in BP.[9a] Compared to bare BP, the A^1_g,

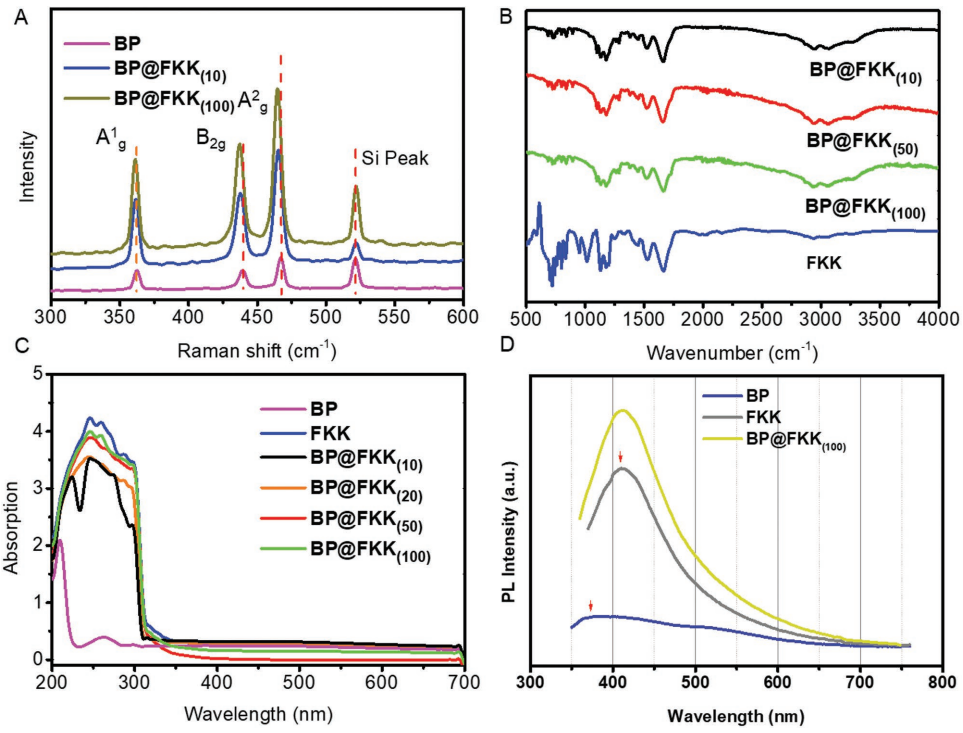

Figure 1. A) Raman spectrum of bare BP and BP@FKK nanosheets. Compared to bare BP, the A^1_g, B_{2g}, and A^2_g modes of BP@FKK were red-shifted. B) FTIR of bare BP and BP@FKK. There was no P—O or P=O stretching modes in the spectra of BP@FKK. C) UV–vis absorption spectrum of bare BP and BP@FKK. D) PL spectrum of BP@FKK nanosheets at excitation wavelength of 325 nm.

B_{2g}, and A^2_g modes of BP@FKK were red-shifted, verifying that there was the interaction between FKK and BP nanosheets, and the largest amount of red-shift occurred in BP@$FKK_{(100)}$. In addition, there were two broad peaks appearing between 1500 and 2000 cm^{-1} in the Raman spectrum of BP@FKK, and the peak positions correspond to the two obvious peaks of FKK as showed in Figure S1 (Supporting Information). This phenomenon approved that the BP nanosheets have been modified with FKK. Figure 1B shows Fourier transform infrared spectroscopy (FTIR) spectrum for FKK, BP@$FKK_{(10)}$, BP@$FKK_{(50)}$ (mass ratio, 1:50), and BP@$FKK_{(100)}$ after being exposed in ambient conditions for 2 days.

In the FTIR spectrum of BP@FKK nanosheets (Figure 1B), the obvious peaks that appeared at 1204 and 1675 cm^{-1} were consistent with the characteristic peaks of Lys and Phe in FKK, respectively. This result showed that BP had been modified with FKK. Furthermore, there was no obvious peak which was corresponding to PO_x derivatives,[8d,15] and this could be caused by the improved stability of BP@FKK nanosheets. However, the dosage of FKK was much more than BP nanosheets, and thus the signal was much stronger; thus the P—O and P=O modes might be covered up. Therefore, we further verify the stability of BP@FKK nanosheets through other characterization methods.

Figure 1C shows the UV–vis absorbance spectrum of bare BP, BP@$FKK_{(10)}$, BP@$FKK_{(20)}$ (mass ratio, 1:20), BP@$FKK_{(50)}$, BP@$FKK_{(100)}$ nanosheets, and free FKK at 200–700 nm wavelength, respectively. The bare BP nanosheets showed broad absorption from UV to visible light region (200–700 nm), and the absorption peak appeared in 200–220 nm. In contrast, the absorption peaks of BP@FKK nanosheets were very close to FKK, and the peak widths were broader from 200 to 300 nm. This result showed that the FKK are introduced to the surface of BP@FKK nanosheets. Additionally, we can see from the UV–vis spectrum that the FKK is saturated when the mass ratio of FKK versus BP reaches 100:1.

In order to detect the fluorescence properties of BP, we referred to the work of Lee,[5a] and the photoluminescence (PL) spectra of free FKK, bare BP, and BP@$FKK_{(100)}$ nanosheets were recorded at 325 and 450 nm excitation wavelengths. As showed in Figure 1D and Figure S2 (Supporting Information), strong emission peaks at about 400 and 550 nm were plotted in the PL spectra. From the spectra, we found that the fluorescence emission of FKK was much stronger than bare BP. The fluorescence of the BP@$FKK_{(100)}$ showed the sum of the FKK and BP. These results further demonstrated the successful modification of FKK on the BP. The strong fluorescence emission of the BP@$FKK_{(100)}$ complex indicated the great potential in bioimaging.

The morphology and crystal structures of bare BP nanosheets and BP@FKK nanosheets were investigated using scanning electron microscope (SEM) and transmission electron microscopy (TEM). The SEM images are shown in Figure S3 (Supporting Information), and these images were acquired in less than 40 s to mitigate sample charging and electron-beam-induced deposition of carbon.

A representative TEM image of few layered bare BP nanosheets with lateral dimensions of approximately 500 nm can be observed in **Figure 2**A. After exposed in ambient conditions for 2 days, many holes appeared on the surface of the bare BP nanosheets because of their weak stability. In contrast, as can be seen in Figure 2B, there was no apparent change appearing on the BP@$FKK_{(100)}$ nanosheets under the same condition. The successful modification of FKK on BP nanosheets was further confirmed by this phenomenon. The crystal structures of bare BP and BP@$FKK_{(100)}$ nanosheets were consistently verified by using high-resolution TEM (HRTEM) imaging (Figure 2C,D) and selected area electron diffraction (SAED) (inset in Figure 2D). The HRTEM image in Figure 2D showed lattice fringes of 0.34 nm, which were ascribed to the (021) plane of the BP crystal.[4a] It has been further confirmed that the BP nanosheets remain the orthorhombic structure of BP after modified by FKK.

High-resolution X-ray photoelectron spectroscopy (HRXPS) was performed to assess the chemical quality of the bare

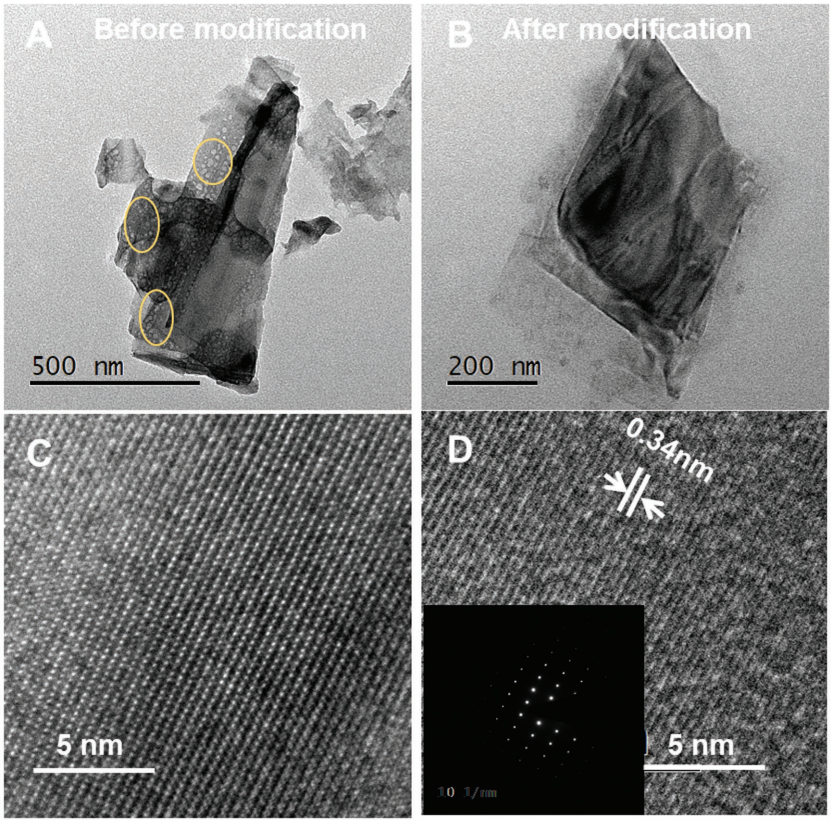

Figure 2. A,B) The TEM figures of bare BP and BP@$FKK_{(100)}$ nanosheets. C,D) HRTEM patterns of bare BP and BP@$FKK_{(100)}$ nanosheets, the inset in (D) is the SAED pattern of the BP@$FKK_{(100)}$.

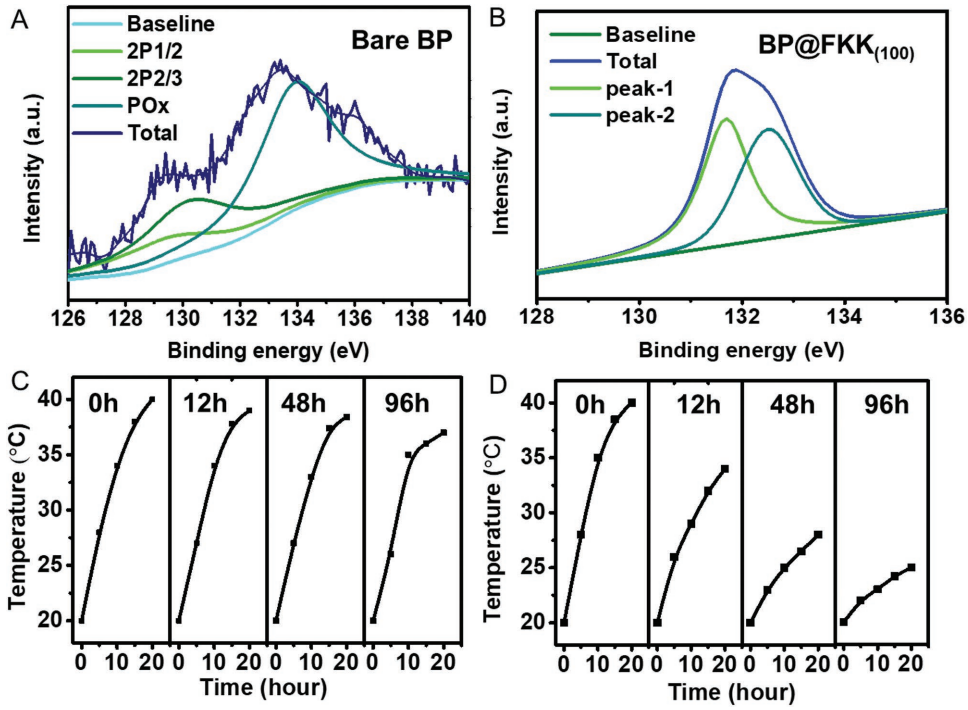

Figure 3. High-resolution XPS spectra of A) bare BP nanosheets and B) BP@FKK$_{(100)}$. The bare BP nanosheets exhibited three characteristic binding energy peaks corresponding to P2$_{p3/2}$, P2$_{p1/2}$, and P_xO_y. However, no P_xO_y peak can be observed from BP@FKK$_{(100)}$, and the other two peaks position have changed. Photothermal heating curves of C) bare BP and D) BP@FKK$_{(100)}$ dispersed in water after exposure to air for 0, 12, 48, and 96 h using the 808 nm laser as the irradiation source. The photothermal performance of BP@FKK$_{(100)}$ was much better than bare BP.

BP and BP@FKK$_{(100)}$ (**Figure 3**A,B; Figure S4, Supporting Information). As shown in Figure 3A, bare BP nanosheets exhibited the P2$_{p3/2}$ and P2$_{p1/2}$ at 130.1 and 130.9 eV, respectively, which are the characteristics of crystalline BPs based on previous reports.[4b,8d] In addition, intense oxidized phosphorus (P_xO_y) sub-bands emerged at 134.0 eV indicating partial oxidization of BP during exposure to air. This phenomenon has been observed from bare BP by XPS.[4b,7] In contrast, no P_xO_y peak was observed from BP@FKK$_{(100)}$ in Figure 3B, indicating better stability of BP@FKK$_{(100)}$ against oxidization than bare BP. Furthermore, in BP@FKK$_{(100)}$ nanosheets, there were two binding energy peaks which appeared at 131.7 and 132.5 eV. The shift of these two peaks may be attributed to the interaction between FKK and BP. The XPS thus confirmed successful modification of FKK to BP in BP@FKK nanosheets.

Recently, great attention has been paid to the photothermal agent BP which can convert near-infrared (NIR) light into heat in photothermal cancer therapy.[2b] When used in medical applications, BP@FKK nanosheets must have enough photothermal stability to deal with long exposure in humid environment. Figure 3C,D shows the result of the photothermal stability comparison between bare BP and BP@FKK$_{(100)}$ nanosheets (both of them were dispersed in water). According to the test data obtained by an infrared thermal imaging camera, the relation curves of solution temperature after light treatment and exposure time were presented. After laser irradiation for 20 min, the freshly prepared solution temperature of the bare BP nanosheets increased from 20 to 40 °C (Figure 3C). It proved that BP nanosheets can convert NIR light into heat. After 96 h exposure to air, the temperature of the bare BP nanosheets solution merely increased to 25°C with 20 min irradiation. The photothermal performance of BP@FKK$_{(100)}$, by contrast, was much better (Figure 3D). After 96 h, the photothermal test result was that the temperature of the BP@FKK solution increased to 37.5 °C with 20 min irradiation. To further study the morphology changes after the laser irradiation in the TEM images, the morphology and crystal structures of bare BP nanosheets and BP@FKK nanosheets were investigated after exposure to air for 96 h followed by the photothermal performance test using TEM (Figure S5, Supporting Information). As Figure S5A (Supporting Information) shows, many holes appeared on the surface of the bare BP and the edge was blurred. In contrast, the morphology and crystal structures of BP@FKK remained intact under the same condition (Figure S5B,D, Supporting Information). Figure S6 (Supporting Information) shows the photothermal heating curves of free FKK, bare BP, and BP@FKK nanosheets with various FKK concentration dispersed in phosphate-buffered saline (PBS) solution. The temperature rises in BP@FKK solutions were about fourfold to fivefold higher than those of FKK, which showed almost no difference with BP. Notably, the influence of FKK on the photothermal effect of BP was negligible.

The average size of BP nanosheets dispersed in the ethanol solution (0.1 mg mL^{-1}) was detected (**Figure 4**A). The average diameter increased from 650 to 1460 nm with the feeding ratio of FKK and BP increased from 0 to 100:1. The zeta potential test showed that the surface potential of BP nanosheets

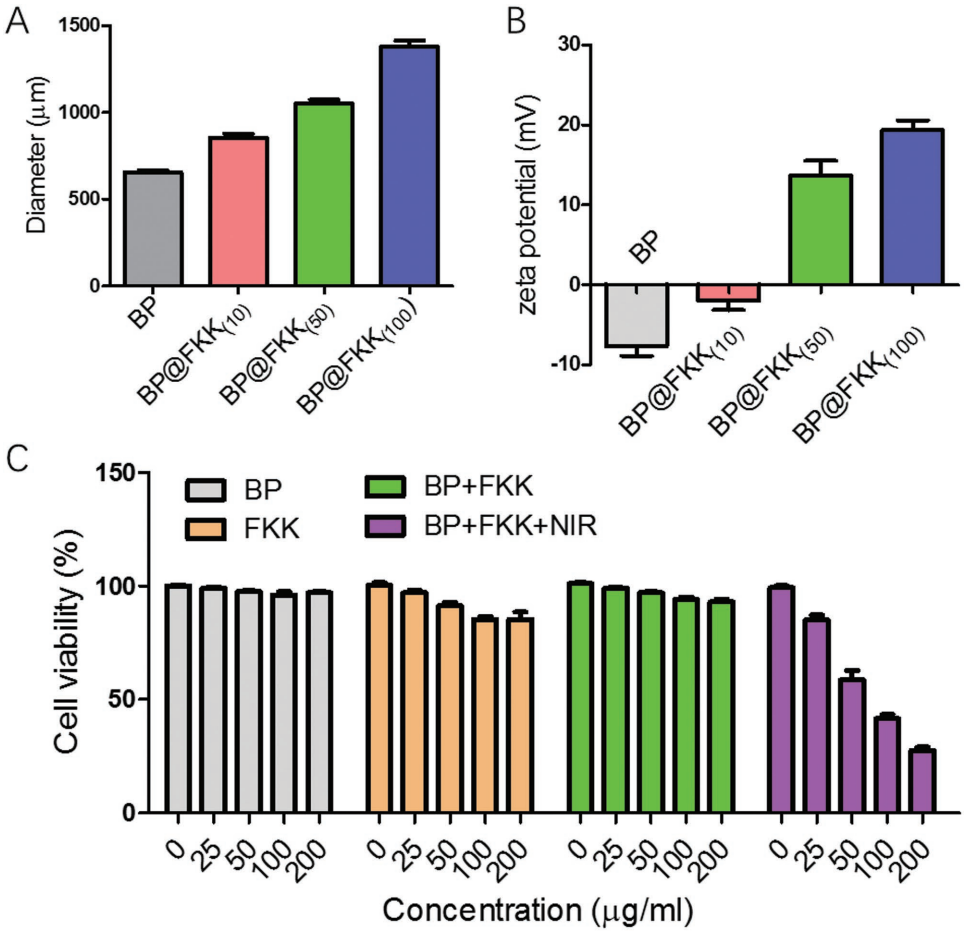

Figure 4. A) Dynamic light scattering measurement of the diameters of BP and BP@FKK complexes. B) Surface zeta potential of BP and BP@FKK nanosheets. C) Cell viability of Hela cells treated with bare BP, FKK, BP@$FKK_{(100)}$, or BP@$FKK_{(100)}$+NIR nanosheets for 48 h at 37 °C. For the group (BP@$FKK_{(100)}$+NIR), the NIR light was applied at 4 h after incubation and the illumination last for 1 h.

was increased from −8.5 to +19 mV after modifying with FKK (Figure 4B), and the values were positively augmented with the peptide concentration increased. These changes could be ascribed to the positively charged FKK immobilized onto the negatively charged BP nanosheets. In addition, the 3-(4,5-dimethyl-2-thiazolyl)-2,5-diphenyl-2-H-tetrazolium bromide (MTT) assay was performed to study the cytotoxicity of BP@FKK on cells in vitro. Hela cells were incubated with free FKK, bare BP, or BP@$FKK_{(100)}$ nanosheets for 72 h in 37 °C. All the samples used in the test had little influence on the viability of Hela cells. While illuminated by the 808 nm laser, the viability of the Hela cells treated with BP@$FKK_{(100)}$ nanosheets was significantly inhibited in a concentration-dependent manner. In contrast, another group of Hela cells cocultured with different concentrations of bare BP nanosheets retained high activity after the same laser illumination. Figure S7 (Supporting Information) showed the comparison of cell viability of Hela cells treated with BP+NIR or BP@$FKK_{(100)}$+NIR nanosheets for 48 h at 37 °C. To this end, we successfully demonstrated that BP@FKK was biocompatible and may be used for photothermal cancer therapy in future.

To investigate the cellular uptake ability of BP and BP@FKK by cancer cells, the flow cytometry (FACS) measurement and confocal microscopy imaging were conducted (**Figure 5**). Before the characterization, Hela cells were cultured with bared BP or BP@FKK for 4 h at 37 °C. As the BP and BP@FKK exhibited PL emission from 400 to 800 nm in the PL measurement, the intracellular fluorescence of BP@FKK under a UV (365 nm) excitation were recorded. As shown in Figure 5A,B, flow cytometry results confirmed that fluorescence intensity of Hela cells increased after incubated with BP@FKK, and the values were positively augmented with the peptide content increase. For the confocal microscopy results, as Figure 5C shows, a blue color was emitted in the Hela cells under UV light excitation when treated with BP@FKK. The strongest fluorescence intensity was obtained at the BP@$FKK_{(100)}$ group, and the blue fluorescence presented in some nucleus. In contrast, the group treated with bare BP nanosheets emitted no fluorescence. This phenomenon indicated that after modified with FKK, the cellular even the nucleus uptake ability of the BP nanosheets were enhanced. The difference in the fluorescence performance between the bare BP and BP@FKK was consistent with the flow cytometer results. Therefore, the BP@FKK nanosheets can be utilized in biomedical applications as a blue emission bioimaging probe and a vehicle for kinds of drug transportation.

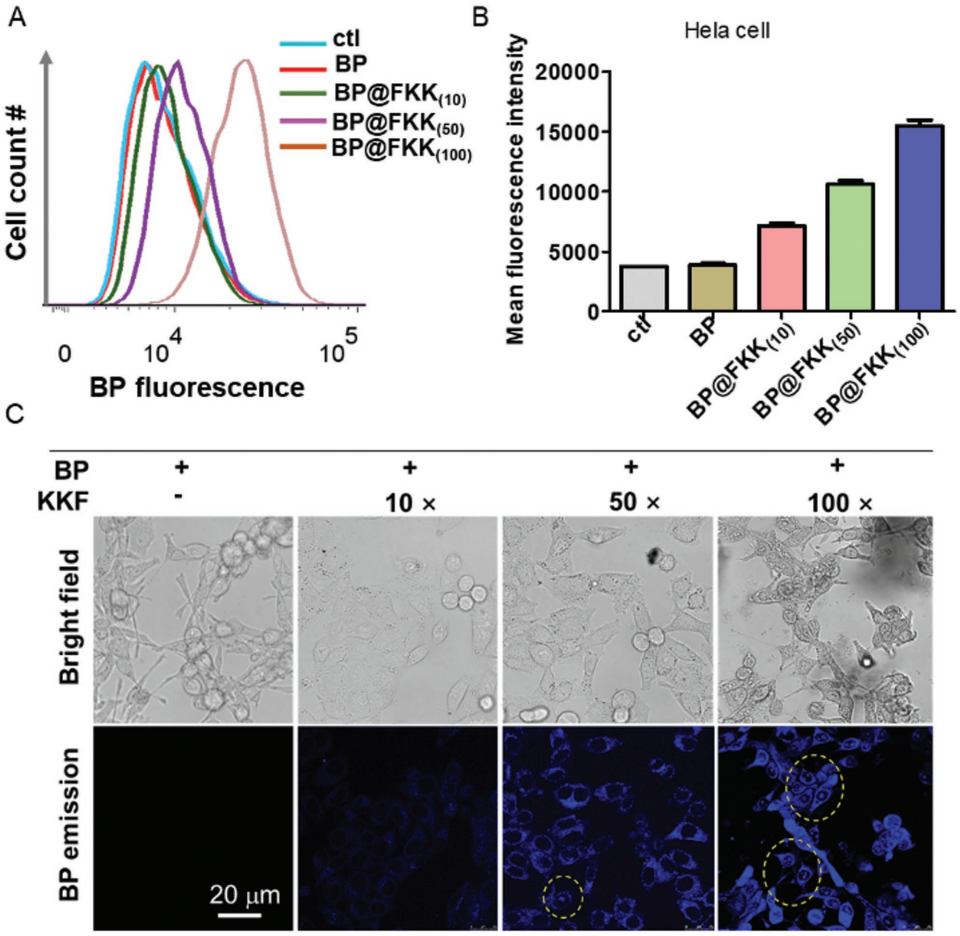

Figure 5. A,B) The cellular fluorescence in Hela cells measured by flow cytometry after treated with bared BP (1 mg mL^{-1}), $BP@FKK_{(10)}$ (1 mg mL^{-1}), $BP@FKK_{(50)}$ (1 mg mL^{-1}), and $BP@FKK_{(100)}$ (1 mg mL^{-1}) for 4 h at 37 °C, the normal cells were utilized as a control. The (B) figure is the statistics of average fluorescence intensity in cells. C) Live cell confocal microscopy images of Hela cells after 4 h incubation with bared BP and BP@FKK at 37 °C. The upper row is bright field (BF) images and the second row is fluorescence images. All scale bars in these images were 20 μm.

In conclusion, our findings provide a simple and efficient strategy to enhance the stability of BP against oxidation and degradation. Due to the inherent attributes of short peptides such as biocompatibility, chemical versatility, biological recognition abilities, and facile synthesis, we chose a simple tripeptide FKK and studied the effect of its stabilization of BP for the first time. We hypothesized that the interaction mode between FKK and BP is through π–p interaction or electrostatic attraction or both exist. The detailed mechanism of passivating the lone-pair electrons of the P atoms to make BP more stable in BP@FKK needs further careful study. Furthermore, we have demonstrated the BP@FKK with excellent stability in vitro, persistent fluorescence intensity, great photothermal effect, and high biocompatibility, which endow the BP@FKK nanosheets with many potential applications as a robust platform for the biomedical uses such as drug delivery or cellular tracking systems.

Supporting Information

Supporting Information is available from the Wiley Online Library or from the author.

Acknowledgements

H.Y.W., K.H., and Z.L. contributed equally to this work. This work was supported by the national key R&D project from Minister of Science and Technology, China (2016YFA0202703), NSFC (31571006, 81601629, 61501039), Beijing Talents Fund (2015000021223ZK21), the Beijing Natural Science Foundation (2182091, 2162017) and "Thousands Talents" program for pioneer researcher and his innovation team.

Conflict of Interest

The authors declare no conflict of interest.

Keywords

biocompatibility, black phosphorus, peptide, photothermal, stability

Received: May 3, 2018
Revised: June 5, 2018
Published online:

[1] a) H. O. Churchill, P. Jarillo-Herrero, *Nat. Nanotechnol.* **2014**, *9*, 330; b) H. Liu, A. T. Neal, *ACS Nano* **2014**, *8*, 4033; c) L. Li, Y. Yu,

G. J. Ye, Q. Ge, X. Ou, H. Wu, D. Feng, X. H. Chen, Y. Zhang, *Nat. Nanotechnol.* **2014**, *9*, 372; d) G. Qin, Q. B. Yan, Z. Qin, S. Y. Yue, H. J. Cui, Q. R. Zheng, G. Su, *Sci. Rep.* **2015**, *4*, 6946; e) H. Liu, Y. Du, Y. Deng, P. D. Ye, *Chem. Soc. Rev.* **2015**, *44*, 2732; f) F. Xia, H. Wang, Y. C. Jia, *Nat. Commun.* **2014**, *5*, 4458.

[2] a) A. S. Moghaddam, C. C. Mayorga-Martinez, Z. Sofer, D. Bouša, E. Saievar-Iranizad, M. Pumera, *J. Phys. Chem. C* **2017**, *121*, 20532; b) C. M. Park, H. J. Sohn, *Adv. Mater.* **2007**, *19*, 2465.

[3] C. C. Mayorga-Martinez, Z. Sofer, *Angew. Chem., Int. Ed.* **2015**, *54*, 14317.

[4] a) P. Yasaei, B. Kumar, T. Foroozan, C. Wang, M. Asadi, D. Tuschel, J. E. Indacochea, R. F. Klie, A. Salehi-Khojin, *ACS Nano* **2015**, *4*, 3596; b) J. Kang, J. D. Wood, S. A. Wells, J. H. Lee, X. Liu, K. S. Chen, M. C. Hersam, *ACS Nano* **2015**, *9*, 3596.

[5] a) H. U. Lee, S. Y. Park, S. C. Lee, S. Choi, S. Seo, H. Kim, J. Won, K. Choi, K. S. Kang, H. G. Park, H. S. Kim, H. R. An, K. H. Jeong, Y. C. Lee, J. Lee, *Small* **2016**, *12*, 214; b) W. Chen, J. Ouyang, H. Liu, M. Chen, K. Zeng, J. Sheng, Z. Liu, Y. Han, L. Wang, J. Li, L. Deng, Y. N. Liu, S. Guo, *Adv. Mater.* **2017**, *29*, 1603864; c) W. Tao, X. Zhu, X. Yu, X. Zeng, Q. Xiao, X. Zhang, X. Ji, X. Wang, J. Shi, H. Zhang, L. Mei, *Adv. Mater.* **2017**, *29*, 1603276; d) H. Wang, X. Yang, W. Shao, S. Chen, J. Xie, X. Zhang, J. Wang, Y. Xie, *J. Am. Chem. Soc.* **2015**, *137*, 11376; e) C. Sun, L. Wen, J. Zeng, Y. Wang, Q. Sun, L. Deng, C. Zhao, Z. Li, *Biomaterials* **2016**, *91*, 81.

[6] G. Qu, W. Liu, Y. Zhao, J. Gao, T. Xia, J. Shi, L. Hu, W. Zhou, J. Gao, H. Wang, Q. Luo, Q. Zhou, S. Liu, X. Yu, G. Jiang, *Angew. Chem., Int. Ed.* **2017**, *56*, 14488.

[7] Z. Sun, H. Xie, S. Tang, X. F. Yu, Z. Guo, J. Shao, H. Zhang, H. Huang, H. Wang, P. K. Chu, *Angew. Chem., Int. Ed.* **2015**, *54*, 11526.

[8] a) H. Liu, A. T. Neal, Z. Zhu, Z. Luo, X. Xu, D. Tomanek, P. D. Ye, *ACS Nano* **2014**, *8*, 4033; b) M. Buscema, D. J. Groenendijk, S. I. Blanter, G. A. Steele, H. S. van der Zant, A. Castellanos-Gomez, *Nano Letters* **2014**, *14*, 3347; c) A. Favron, E. Gaufrès, F. Fossard, A. L. Phaneuf-L'Heureux, N. Y. Tang, P. L. Lévesque, A. Loiseau, R. Leonelli, S. Francoeur, R. Martel, *Nat. Mater.* **2015**, *14*, 826; d) J. D. Wood, S. A. Wells, D. Jariwala, K. S. Chen, E. Cho, V. K. Sangwan, X. Liu, L. J. Lauhon, T. J. Marks, M. C. Hersam, *Nano Letters* **2014**, *14*, 6964; e) J. S. Kim, Y. Liu, W. Zhu, S. Kim, D. Wu, L. Tao, A. Dodabalapur, K. Lai, D. Akinwande, *Sci. Rep.* **2015**, *5*, 8989.

[9] a) R. A. Doganov, E. C. O'Farrell, S. P. Koenig, Y. Yeo, A. Ziletti, A. Carvalho, D. K. Campbell, D. F. Coker, K. Watanabe, T. Taniguchi, A. H. Castro Neto, B. Özyilmaz, *Nat. Commun.* **2015**, *6*, 6647; b) B. Wan, B. Yang, Y. Wang, J. Zhang, Z. Zeng, Z. Liu, W. Wang, *Nanotechnology* **2015**, *26*, 435702.

[10] Z. Guo, S. Chen, Z. Wang, Z. Yang, F. Liu, Y. Xu, J. Wang, Y. Yi, H. Zhang, L. Liao, P. K. Chu, X. F. Yu, *Adv. Mater.* **2017**, *29*, 1703811.

[11] C. R. Ryder, J. D. Wood, S. A. Wells, Y. Yang, D. Jariwala, T. J. Marks, G. C. Schatz, M. C. Hersam, *Nature Chemistry* **2016**, *8*, 597.

[12] Y. Zhao, H. Wang, H. Huang, Q. Xiao, Y. Xu, Z. Guo, H. Xie, J. Shao, Z. Sun, W. Han, X. F. Yu, P. Li, P. K. Chu, *Angew. Chem., Int. Ed.* **2016**, *55*, 5003.

[13] A. Ziletti, A. Carvalho, D. K. Campbell, D. F. Coker, A. H. Castro Neto, *Phys. Rev. Lett.* **2015**, *114*, 046801.

[14] a) C. Hao, B. Yang, F. Wen, J. Xiang, L. Li, W. Wang, Z. Zeng, B. Xu, Z. Zhao, Z. Liu, Y. Tian, *Adv. Mater.* **2016**, *28*, 3194; b) S. Lin, Y. Chui, Y. Li, S. P. Lau, *Chem* **2017**, *2*, 15.

[15] A. Rosemary, L. C. Thomas Chittenden, *Spectrochim. Acta* **1965**, *21*, 861.